Turbulence, Heat and Mass Transfer 6
K. Hanjalić, Y. Nagano and S. Jakirlić (Editors)

A unified model of turbulent mass transfer under different interfacial conditions

Y. Hasegawa[1] and N. Kasagi[2]

[1]*Department of Mechanical Engineering, The University of Tokyo, Hongo 7-3-1, Bunkyo-ku, Tokyo 113-8656, Japan, hasegawa@thtlab.t.u-tokyo.ac.jp*

[2]*Department of Mechanical Engineering, The University of Tokyo, Hongo 7-3-1, Bunkyo-ku, Tokyo 113-8656, Japan, kasagi@thtlab.t.u-tokyo.ac.jp*

Abstract — A theoretical model for predicting the damping of the normal velocity fluctuation close to a contaminated air-water interface is proposed. In the present model, the flow field close to a contaminated interface is approximated by superposition of a free-surface flow at a clean interface and a surfactant-induced flow. It is shown that the present model can predict the normal velocity fluctuation quite well under a wide range of the Marangoni number representing a degree of surface contamination. Finally, the predicted interface-normal velocity fluctuation is used to evaluate the interfacial mass transfer.

1. Introduction

Turbulent mass transfer across an air-water interface plays critical roles in geophysical and industrial processes. In general, except for highly soluble or reactive gases, the most mass transfer resistance exists on the water side. Furthermore, since the Schmidt number of a solute becomes extremely high ($Sc \sim O(10^3)$) in water, a thin concentration boundary layer is formed beneath the interface (Jähne and Hauβecker, 1998). Thus, it is important to understand and even control the microscopic transport mechanism in this concentration boundary layer.

In natural waters, surfactants are commonly present due to machine lubricants, excretion and degradation products of phytoplankton and so forth (Frew, 1997). Generally, the presence of surfactants creates non-uniform surface tension, by which eddying motion approaching the interface is impeded. As a result, the free-surface turbulence and associated interfacial mass transfer are significantly retarded. The closed-loop nature between the surfactant distribution, surface tension and free-surface turbulence makes the process quite complicated.

Recently, Hasegawa and Kasagi (2008) conducted a series of numerical simulations for high Schmidt number turbulent mass transfer across clean and contaminated free surfaces as well as a solid surface. They observed that, with increasing the Marangoni number representing a degree of surface contamination, the mass transfer rate drastically decreases, and consequently converges to the value at a solid surface. As a result, the Schmidt number dependency of mass transfer rate K switches from $K \propto Sc^{-0.5}$ to $Sc^{-0.7}$. This indicates that a highly contaminated interface is dynamically equivalent to a solid surface in terms of the interfacial mass transfer.

In the present study, we will develop a unified model of turbulent mass transfer, which is applicable to dynamically different interfaces, i.e., clean, contaminated and solid surfaces. Our final goal is to predict substantial decrease in the mass transfer rate due to the surface contamination, and also the transition of the mass transfer mode from free to solid surfaces.

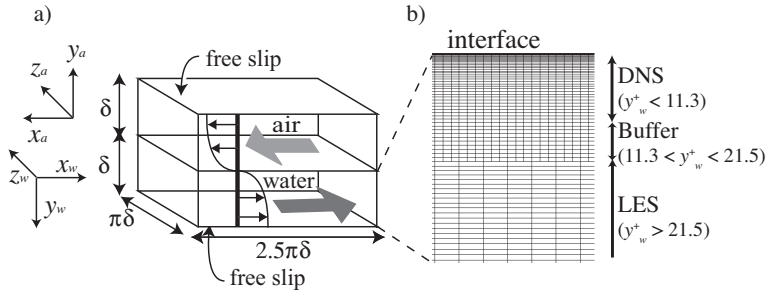

Figure 1: Computational domain and coordinate system

2. Numerical Methods and Conditions

2.1. Velocity field

We consider a counter current air-water flow driven by constant pressure gradient as shown Fig. 1. Throughout this manuscript, x, y, and z represent the streamwise, spanwise and interface-normal directions. The governing equations of the velocity field are the incompressible Navier-Stokes and the continuity equations:

$$\frac{\partial u_i}{\partial t} + \frac{\partial (u_j u_i)}{\partial x_j} = -\frac{\partial p}{\partial x_i} + \frac{1}{Re_\tau}\frac{\partial^2 u_i}{\partial x_j \partial x_j}, \tag{1}$$

$$\frac{\partial u_i}{\partial x_i} = 0. \tag{2}$$

All variables are normalized by the depth δ^* and the friction velocity u_τ^* in each phase. A value with an asterisk represents a dimensional quantity. The Reynolds number based on u_τ^* and δ^* in each phase is $Re_{\tau a}$ = $Re_{\tau w}$ = 150, which corresponds to an air-water flow at a wind speed of 2 m/s at $y_a^* = \delta^* = 4$ cm under a standard condition. The subscripts of a and w represent values in air and water, respectively. The computational periods are $2.5\pi\delta^*$ and $\pi\delta^*$ in the x and z directions, respectively. We confirmed that the extension of the computational domain does not affect the velocity and concentration statistics discussed here. A free-slip condition is imposed at the outer boundaries, i.e., $y_a = y_w = 1.0$, in both phases.

A pseudo-spectral method is applied for spatial discretization. 64 x 64 Fourier modes and 128 Chebyshev polynomials are used in the horizontal and normal directions, respectively. Computation with doubled modes in each direction was conducted to ensure that the present grid system is fine enough to resolve all essential scales of the velocity field. For time integration, the second-order Adams-Bashforth scheme is adopted for the advection terms, while the Crank-Nicolson scheme for the viscous terms.

2.2. Concentration field

The transport equation of the solute concentration c is given by:

$$\frac{\partial c}{\partial t} + \frac{\partial (u_j c)}{\partial x_j} = \frac{1}{ScRe_\tau}\frac{\partial^2 c}{\partial x_j \partial x_j}, \tag{3}$$

where the concentration c is normalized by the concentration difference ΔC^* between the interface and the bottom boundary in the water phase. Since most mass transfer resistance exists on the water side, we solve the concentration field only in the water phase under a constant concentration conditions, i.e., $c = 1.0$ and 0 at the interface and the bottom boundary, respectively.

The Schmidt number $Sc = \nu^*/D^*$ is defined by the kinematic viscosity ν^* and the molecular diffusivity D^* of a solute. In the present study, Sc is changed as 1.0 and 100. In the case of $Sc = 1.0$, the same numerical scheme and grid system as those for the velocity field are used.

In order to calculate the high Schmidt number concentration field at $Sc = 100$, we employ a hybrid DNS/LES scheme, which applies direct numerical simulation (DNS) with high-resolution grids within the near-interface region, while large-eddy simulation (LES) with coarser grids in the outer layer as shown in Fig. 1b). Details of the numerical scheme can be found in Hasegawa and Kasagi (2009).

2.3. Interfacial dynamical condition

Since we focus on the effects of interfacial dynamical condition on the mass transfer, the interface is assumed to be flat for simplicity, i.e., v_w = v_a = 0. The resultant interfacial boundary conditions for the velocity field are the continuity of velocity components and the balance of the shear stress and the surface tension in the tangential directions. They are written in dimensionless forms as:

$$u_{wj} = \sqrt{\frac{\rho_w^*}{\rho_a^*}} u_{aj}, \tag{4}$$

$$\frac{1}{Re_{\tau w}} \frac{\partial u_{wj}}{\partial x_2} = \frac{1}{Re_{\tau a}} \frac{\partial u_{aj}}{\partial x_2} - \frac{1}{We} \frac{\partial \sigma}{\partial x_j} \tag{5}$$

where $j = 1$ or 3. The surface tension σ is normalized by the equilibrium surface tension σ_0^*. The Weber number is defined by $We = \tau^* \delta^* / \sigma_0^*$, where $\tau^* = \rho_w^* {u_{\tau w}^*}^2 = \rho_a^* {u_{\tau a}^*}^2$ is the interfacial shear stress. For simplicity, we assume the following linear relationship between the surface tension σ and the surfactant concentration γ:

$$\sigma - 1 = Ma(1 - \gamma). \tag{6}$$

Here, γ is normalized by the equilibrium concentration γ_0^*. The Marangoni number is defined by $Ma = -(\gamma_0^*/\sigma_0^*)(d\sigma^*/d\gamma^*)_{\gamma=1}$. By substituting Eq. (6), the interfacial boundary condition (5) results in:

$$\frac{1}{Re_{\tau w}} \frac{\partial u_{wj}}{\partial x_2} = \frac{1}{Re_{\tau a}} \frac{\partial u_{aj}}{\partial x_2} + \frac{Ma}{We} \frac{\partial \gamma}{\partial x_j}. \tag{7}$$

In the present study, We is kept constant as $We = 9.0 \cdot 10^{-4}$, while Ma is systematically changed as $Ma = 0$ (Clean), $1.0 \cdot 10^{-3}$ (Case 1), $1.0 \cdot 10^{-2}$ (Case 2) and $1.0 \cdot 10^{-1}$ (Case 3). Note that $Ma = 0$ corresponds to a clean interface.

The transport equation of an insoluble surfactant concentration γ in the two-dimensional interface gives rise to:

$$\frac{\partial \gamma}{\partial t} + \frac{\partial (u_w \gamma)}{\partial x} + \frac{\partial (w_w \gamma)}{\partial z} = \frac{1}{Sc_\gamma Re_{\tau w}} \left(\frac{\partial^2 \gamma}{\partial x^2} + \frac{\partial^2 \gamma}{\partial z^2} \right). \tag{8}$$

Note that the total amount of the surfactant on the interface is always conserved. The Schmidt number of the surfactant is $Sc_\gamma = 1.0$ in all cases.

The whole computation proceeds as follows. The Navier-Stokes and continuity equations (1) and (2) in the air and water phases are solved by a pseudo-spectral method under the coupled interfacial conditions (4) and (7). Similarly, the transport equation (3) of a solute concentration

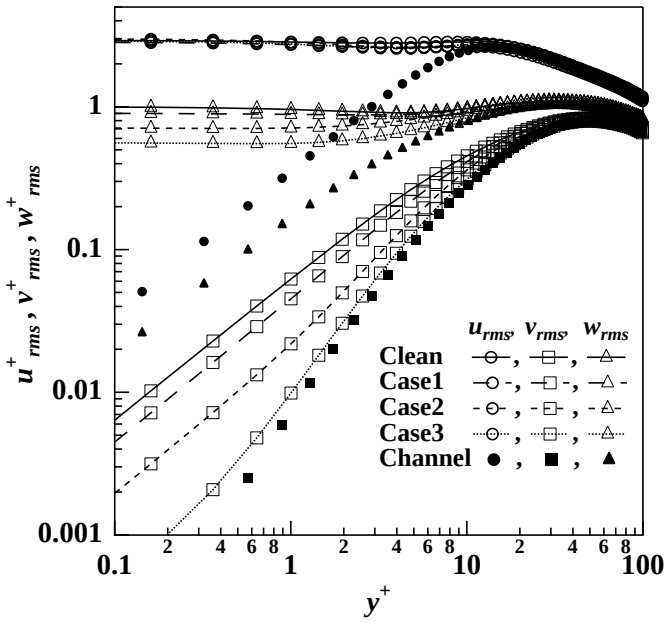

Figure 2: Velocity fluctuations near the interface in the water phase

c is solved in the water phase. The obtained velocity field at the interface is used for solving the surfactant transport equation (8). The resultant surfactant concentration γ is assigned to the interfacial boundary condition (7) in the next step.

3. Results

3.1. Velocity field

Since the interface is dynamically similar to a solid surface for the air flow due to large density ratio between water and air, and the most mass transfer resistance exists on the water side, we focus on the surfactant effects on the flow statistics on the water side.

The velocity fluctuations near the interface are shown in Fig. 2. It is found that the streamwise and spanwise velocity fluctuations are kept almost unchanged, while only the normal velocity fluctuation is damped drastically with increasing the Marangoni number. This indicates that the velocity field near a highly contaminated interface is essentially different from that near a solid surface. As will be discussed in the following subsection, the drastic damping of the normal velocity fluctuation is a primary reason for the change of mass transfer mode at a contaminated interface. Other fundamental statistics of the velocity field were reported in Hasegawa and Kasagi (2008).

3.2. Concentration field

The mass transfer rate K^+ in the water phase is defined by:

$$K^+ = \frac{Q^*}{u^*_{\tau w}(C^*_I - C^*_B)} = \frac{1}{\Delta C^+_B}. \tag{9}$$

Here, C^*_I and C^*_B are the mean concentration at the interface and the bulk, respectively, while $\Delta C^*_B = C^*_I - C^*_B$. The mass transfer rates at $Sc = 1.0$ and 100 in all cases are plotted in Fig. 3. With increasing the Marangoni number, K^+ is drastically decreased, and eventually converges

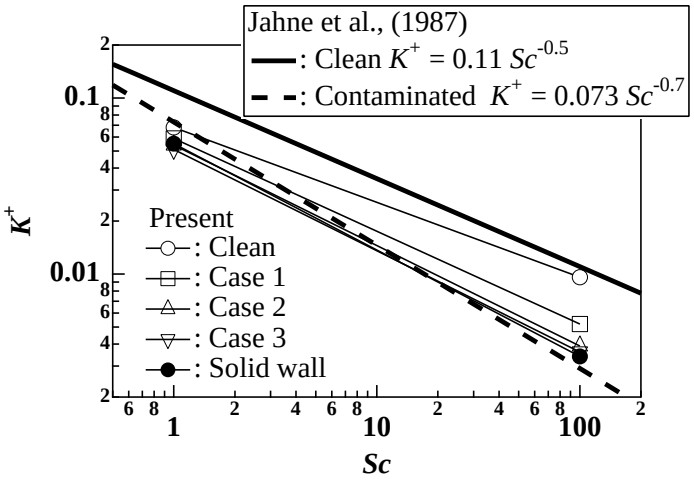

Figure 3: Mass transfer rates as a function of the Schmidt number

to the value at a solid surface. Surface contamination has a profound effect at the high Schmidt number, since the most resistance to mass transfer lies in a thinner layer beneath the interface.

Jähne et al. (1987) compiled experimental data and showed that K is correlated as $K^+ = 0.11Sc^{-0.5}$ and $0.073Sc^{-0.7}$ for clean and highly contaminated interfaces, respectively. The present numerical results agree well with the experimental data. It should be noted that the change of the Schmidt number dependency of K is also well reproduced. This suggests that the mass transfer mode switches to that near a solid surface at highly contaminated interfaces, i.e., Cases 2 and 3.

In the following section, we will develop a mass transfer model with particular attention to the damping of the normal velocity fluctuation at a contaminated interface.

4. Mass Transfer Model

4.1. Modeling of concentration boundary layer

Considering the concentration boundary layer becomes extremely thin at high Schmidt numbers, the concentration filed near a free or solid surface can be well approximated by the following one-dimensional advection-diffusion equation:

$$\frac{\partial c^+}{\partial t^+} + v^+ \frac{\partial c^+}{\partial y^+} = \frac{1}{Sc} \frac{\partial^2 c^+}{\partial y^{+2}} \tag{10}$$

The interface-normal velocity v can be represented by Taylor series as $v(y,t) = -\beta(t)y$ and $v(y,t) = \eta(t)y^2$ near free and solid surfaces, respectively. Here, β is the surface divergence and defined as $\beta = -(\partial v/\partial y)_{y=0} = (\partial u/\partial x + \partial w/\partial z)_{y=0}$. Hasegawa and Kasagi (2008) showed that, for a clean or slightly contaminated interface, the mass transfer rate K can be well correlated by the following equation:

$$K^+ = K^*/u^*_{\tau w} = 0.4\sqrt{\frac{\beta^+_{rms}}{Sc}} \tag{11}$$

A theoretical support for this model is extensively discussed in Hasegawa and Kasagi (2009). With increasing the surface contamination, however, β rapidly decreases, and eventually the quadratic term in y becomes dominant. In this case, K is no longer related to β and converges

to the value at a solid surface. These results indicate that the normal velocity fluctuation close to a contaminated interface is a key for predicting the mass transfer.

4.2. Modeling of viscous sublayer

According to Fig. 2, the damping of velocity fluctuations due to surface contamination mainly occurs inside the viscous sublayer. Hence, we assume that the surface contamination influences the flow field through viscosity, and the non-linear interaction between the surfactant-driven flow and the outer flow is negligible. As a result, the flow field near a contaminated interface can be modeled as superposition of an original flow near a clean surface and a surfactant-driven viscous flow. Hereafter, the surface divergence at a clean surface is denoted by β_0, while the surface divergence induced by the surfactant is β_s. Thus, the surface divergence β_c at a contaminated interface is given by $\beta_c = \beta_0 + \beta_s$. By applying a two-dimensional divergence operator $\nabla_H = (\partial/\partial x, \partial/\partial z)$ to the linearized Navier-Stokes equation, the following equation for β_s is obtained:

$$\frac{\partial \beta_s}{\partial t} = \frac{1}{Re_\tau} \nabla^2 \beta_s, \tag{12}$$

where the boundary conditions for β_s are deduced from Eq. (7) as:

$$\begin{aligned} \frac{\partial \beta_s}{\partial y} + \frac{MaRe_{tau}}{We} \nabla_H^2 \gamma \quad &= 0 \;\; at \;\; y = 0, \\ \beta_s \quad &= 0 \;\; as \;\; y \to \infty. \end{aligned} \tag{13}$$

Here, $\nabla_H^2 = \partial^2/\partial x^2 + \partial^2/\partial z^2$. By analytically solving Eq. (12) under the boundary conditions (13), the following damping factor D_f, which represents the ratio between the surface divergences at clean and contaminated interfaces is obtained:

$$D_f = \frac{\tilde{\beta}_c}{\tilde{\beta}_0} = 1 - \frac{\tilde{\beta}_s}{\tilde{\beta}_0} = \left(\frac{\sqrt{A}}{B + \sqrt{A}} \right) \left[1 - \left\{ \frac{\sqrt{k_x^2 + k_z^2} B}{\sqrt{A}(B + \sqrt{A})} \right\} \right], \tag{14}$$

where

$$A = i\omega Re_\tau, \quad B = i \frac{MaRe_\tau}{We} \frac{(k_x^2 + k_z^2)}{\omega}. \tag{15}$$

Here, a tilde represents operation of Fourier transform in time t and horizontal directions x and z. The wave numbers in the x and z directions and frequency are denoted by k_x, k_z and ω, respectively. Since the present model is linear, the surface divergence β_c at a contaminated interface can be obtained by simply multiplying the surface divergence β_0 at a clean interface with the damping factor of Eq. (14) for individual wave numers k_x, k_z and frequency ω.

4.3. Model verification

The interface-normal velocity fluctuations at clean, contaminated and solid surfaces obtained by DNS and the present model are compared in Fig. 4. The model predictions show good agreement with the DNS data. Especially, the change from linear to quadratic limiting behavior is reproduced well.

Once the normal velocity fluctuation close to a contaminated interface is obtained, the interfacial mass transfer rate can be calculated by Eq. (11). The mass transfer rate as a function of

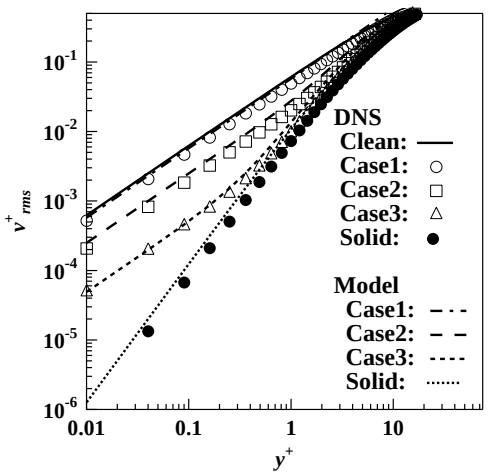

Figure 4: Limiting behavior of normal velocity fluctuation at clean, contaminated and solid surfaces

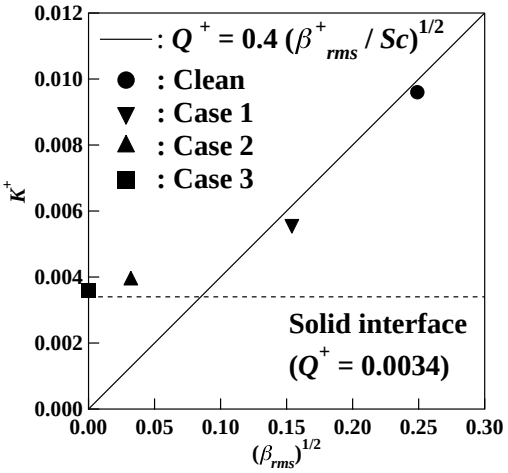

Figure 5: Mass transfer rates at clean and contaminated interfaces as a function of $\sqrt{\beta_{rms}}$

the root mean square of the surface divergence fluctuation is plotted in Fig. 5. For clean and slightly contaminated interfaces (Clean and Case 1), the mass transfer rate shows good agreement with Eq. (11). For highly contaminated interfaces (Cases 2 and 3), the surface divergence becomes vanishingly small. Consequently, the mass transfer rate converges to a lower limit, i.e., the value at a solid surface. The present results indicate that the mass transfer rate and the transition of the mass transfer mode from free to solid surfaces are well predicted by using the intensity of the surface divergence fluctuation.

5. Conclusions

A linear model for predicting the interface-normal velocity fluctuation near a contaminated interface was developed. The damping factor depends on the spatial wave numbers and frequency of the surface divergence fluctuation as well as the Marangoni number representing a degree of surface contamination. Although the present model is a simple linear model, good agreement between the model prediction and the DNS data was confirmed for a wide range of the

Marangoni number. By combining the present model with the surface divergence model (11), it becomes possible to predict the mass transfer rate at a contaminated interface, and also the transition of the mass transfer mode from free to solid surfaces.

6. Acknowledgements

The present work was supported through Grant-in-Aid for Young Scientists (B), 19760131, 2007, by the Ministry of Education, Culture, Sports, Science and Technology, Japan.

References

1. B. Jähne and H. Hauβecker. Hybrid DNS/LES of High Schmidt Number Mass Transfer across Turbulent Air-Water Interface. *Annu. Rev. Fluid Mech.*, 30:443-468, 1998.
2. N. M. Frew. The Role of Organic Films in Air-Sea Gas Exchange In *The Sea Surface and Global Change (Edited by P. S. Liss and R. A. Duce)*, pp. 121-172, Cambridge University Press, 1997.
3. Y. Hasegawa and N. Kasagi. Systematic Analysis of High Schmidt Number Turbulent Mass Transfer across Clean, Contaminated and Solid Interfaces. *Int. J. Heat and Fluid Flow*, 29:765-773, 2008.
4. Y. Hasegawa and N. Kasagi. Hybrid DNS/LES of High Schmidt Number Mass Transfer across Turbulent Air-Water Interface. *Int. J. Heat and Mass Transfer*, 52:1012-1022, 2009.
5. B. Jähne, K. O. Münnich, R. Bösinger, A. Dutzi, W. Huber and P. Libner. On the Prarameters Influencing Air-Water Gas Exchange. *J. Geophys. Res.*, 92:1937-1949, 1987.